

Influence of bacterial uptake on deep-ocean dissolved organic carbon

Jørgen Bendtsen and Claus Lundsgaard

National Environmental Research Institute, Roskilde, Denmark

Mathias Middelboe

Marine Biological Laboratory, University of Copenhagen, Helsingør, Denmark

David Archer

Department of Geophysical Sciences, University of Chicago, Chicago, Illinois, USA

Received 13 June 2002; revised 4 September 2002; accepted 17 September 2002; published 13 December 2002.

[1] Particulate organic carbon (POC) sinking out of the sunlit euphotic zone at the surface of the ocean feeds the deep sea and alters the CO₂ concentration of the atmosphere. Most of the sinking POC is reoxidized to dissolved inorganic carbon (DIC) before it hits the sea floor, but the mechanism for this is poorly understood. Here we develop a global model of the microbial loop in the aphotic zone based on new measurements of deep ocean bacterial metabolism. These together imply that a significant fraction of the decreasing POC flux with depth is converted to dissolved organic carbon (DOC) rather than directly to DIC as is commonly assumed, thereby providing the substrate for free-living bacteria in the deep ocean. The model suggests the existence of a substantial DOC-pool with a relatively fast turnover time in the deep sea. By implementing the microbial loop in a model of the global ocean circulation, we show that the observed gradient of DOC in the deep North Atlantic can be explained by the temperature dependence of bacterial metabolic activity in conjunction with the formation of deep-water at high latitudes. *INDEX TERMS:* 4806 Oceanography: Biological and Chemical: Carbon cycling; 4815 Oceanography: Biological and Chemical: Ecosystems, structure and dynamics; 4840 Oceanography: Biological and Chemical: Microbiology; 4842 Oceanography: Biological and Chemical: Modeling; *KEYWORDS:* dissolved organic carbon, carbon cycle, remineralization, bacteria, microbial loop, Greenland Sea

Citation: Bendtsen, J., C. Lundsgaard, M. Middelboe, and D. Archer, Influence of bacterial uptake on deep-ocean dissolved organic carbon, *Global Biogeochem. Cycles*, 16(4), 1127, doi:10.1029/2002GB001947, 2002.

1. Introduction

[2] DOC in the ocean is mainly of marine origin despite the relatively large fluxes of terrigenous derived organic carbon into the ocean from runoff (0.4 Pg/yr) and aeolian sources [Opsahl and Benner, 1997]. This also holds for the deep-sea DOC in the Greenland Sea where low concentration of lignin oxidation products and high $\delta^{13}\text{C}$ -values of the DOC and the optical properties of the chromophoric dissolved organic matter all indicate a marine biogenic origin of the DOC [Opsahl *et al.*, 1999; Stedmon and Markager, 2001]. The observed concentration of DOC below 1000 m depth is significantly higher in the northern North Atlantic (48–50 μM) than in the rest of the deep ocean (~ 43 μM , except for the northern North Pacific where DOC < 40 μM) [Hansell and Carlson, 1998a]. The deep-sea DOC distribution is also characterized by an old

¹⁴C-age of about 4000–6000 year, which indicates a very low turnover rate of the deep DOC pool [Bauer *et al.*, 1992]. Increased primary production during the spring and summer season causes an accumulation of DOC in the euphotic zone where the surface concentration has been observed to increase by up to 10 μM in the subtropical Atlantic [Carlson *et al.*, 1994] and by 20–30 μM in the Norwegian Sea [Børsheim and Mykkestad, 1997]. Subsequently the accumulated DOC is remineralized or transported into the aphotic zone during the autumn and the winter seasons.

[3] These observations justify a separation of the marine DOC-pool into a “semilabile” and a “refractory” pool with a typical turnover timescale of months and millennia, respectively. This separation of the complex DOC pool into distinct fractions has been used to model the distribution of DOC in the water column. Yamanaka and Tajika [1997] consider a semilabile and a refractory pool of DOC in a global ocean circulation model and they find that the DOC distribution in the upper part of the main thermocline

(0–400 m depth) is well described by an e-folding time for the decay of the semilabile DOC of about 0.5 yr. Due to the short timescale for the decomposition of semilabile DOC into DIC they find that the deep-sea semilabile DOC concentration is only about 1 μM in the deep ocean with a maximum of about 3 μM in the deep northern Pacific. A similar timescale of less than 1 yr for the semilabile DOC is determined in a study of the global carbon cycle where the role of the plankton dynamics in the euphotic zone is explicitly resolved [Six and Maier-Reimer, 1996]. Archer *et al.* [1997] estimate a timescale of about 6 months for the decay of newly produced DOC in the equatorial Pacific which is transported into the seasonal thermocline. In a one-dimensional study of the cycling of labile, semilabile and refractory DOC, the transport by vertical advection and diffusion of DOC was shown to be important in the upper part of the main thermocline whereas the DOC released from the sinking flux of POC was shown to be important for providing the substrate for the bacteria in the deeper part of the water column [Anderson and Williams, 1999]. In accordance with the studies above, Anderson and Williams [1999] estimate a turnover timescale of 0.4 year for the semilabile pool of DOC.

[4] The deep-sea thermohaline circulation in the North Atlantic is dominated by the southward transport of North Atlantic Deep Water (NADW) which originate in the Greenland Sea area [Reid and Lynn, 1971]. Interactions between the thermohaline circulation and the DOC-pool could explain the observed deep-sea gradient of DOC in the North Atlantic, but would imply a timescale for the degradation of DOC of several decades, as this is the timescale for the deep circulation in the eastern North Atlantic [Smethie *et al.*, 2000]. This is much longer than the estimated short timescale of about 6–12 months for the decay of the semilabile fraction of DOC in the tropical and subtropical seasonal thermocline, and significantly less than the timescale for the old “refractory” deep-sea DOC pool. Therefore these models can not explain the observed deep-sea DOC distribution in the North Atlantic reported by Hansell and Carlson [1998a].

[5] Here we show that a simple microbial loop based on the bacterial biomass and the temperature and substrate dependent bacterial metabolic activity can account for the different turnover timescales ranging from months to millennia and that the influence of the bacterial activity is reflected in the deep-sea DOC distribution, in particular in areas close to deep-water formation regions. The microbial loop is based on new measurements from the Greenland Sea which provide evidence for the importance of the particle-associated transport of DOC in the water column. Our results supports the view that a major part of the organic carbon cycle in the ocean may be characterized as: POC \rightarrow DOC \rightarrow Bacteria \rightarrow DIC [Cho and Azam, 1988; Nagata *et al.*, 2000].

2. Measurements of Labile DOC, Bacterial Biomass and Production

[6] We measured the concentration of labile organic carbon and the production and biomass of bacterioplankton during two cruises to the Greenland Sea in June and August

1999 (see Appendix A). Labile DOC (DOC_l) is here defined as the amount of DOC which can be utilized by bacteria within 1 week of incubation at 20°C [Søndergaard and Middelboe, 1995]. DOC_l is not an estimate of the total pool of biodegradable DOC (DOC_b), but provides an estimate of the fraction of DOC_b that is readily utilized by bacteria. Labile DOC was found to be present at significant concentrations of 0.04–0.76 μM below 1000 m depth. We cannot exclude that the measured concentration of labile DOC may be slightly overestimated due to DOC contamination from water filtration and handling of incubation bottles (M. Middelboe and C. Lundsgaard, Microbial activity in the Greenland Sea: The role of DOC lability, mineral nutrients and temperature, submitted to *Aquatic Microbial Ecology*, 2002). However, the fact that we found indications for a well-functioning microbial loop in the deep sea (i.e., significant bacterial production, Table 1) and significant abundance of both viruses and heterotrophic protozoa, supported the observed presence of a pool of labile DOC in the deep waters. The presence of a labile DOC-pool with a turnover time of weeks to months can only be explained by transport via fast sinking (of the order 100 m d^{-1}) particulate organic matter, as any advective or diffusive transport of surface derived DOC to this depth would require several months (see section 5). The bacterial biomass decreases from 11–20 mg C m^{-3} in the upper 100 m to about 4 mg C m^{-3} at 500 m depth and the Production/Biomass (P/B)-ratio decreases correspondingly (Table 1).

3. Microbial Loop

[7] Together with earlier reported observations of the deep-ocean DOC distribution [Hansell and Carlson, 1998a] the observed labile deep-sea DOC-pool in the Greenland Sea motivated the formulation of a model for a microbial loop working in the deep ocean based on the bacterial uptake of particle-transported DOC (Figure 1). The model assumes that all of the sinking POC is dissolved to biodegradable DOC_b through hydrolytic enzymatic activity [Smith *et al.*, 1992; Middelboe *et al.*, 1995], viral lysis of particle-associated bacteria [Proctor and Fuhrman, 1991] or by grazing zooplankton. The dissolution of POC provides the substrate for the free-living bacteria in the deep ocean [Cho and Azam, 1988; Nagata *et al.*, 2000]. Furthermore we assume that the subsequent remineralization of DOC_b ultimately is controlled by the bacterial activity. The deep sea is resource-limited with respect to the supply of organic carbon [Billen *et al.*, 1990; Dufour and Torrèton, 1996; Nagata *et al.*, 2000]; therefore we neglect the effects of viruses, bacterivores and other grazers in controlling the uptake of DOC_b in our model of the mesopelagic zone. Bacterial carbon uptake is determined from our observations of bacterial growth rates and bacterial growth efficiency, and bacterial mortality is constrained by previously reported observations of bacterial abundance and the dissolution of POC to DOC_b in the deep-ocean (see below).

3.1. Model Description

[8] The microbial loop working in the water column below the euphotic zone is driven by the dissolution (D) of the sinking POC to DOC_b (Figure 1). The growth of the

Table 1. Bacterial Biomass, Production, P/B-Ratios and Labile DOC in the Greenland Sea^a

Depth, m	T, °C	N	B, mgC m ⁻³	P, 10 ⁻⁵ gC m ⁻³ d ⁻¹	μ, 10 ⁻² d ⁻¹	n	⟨DOC _l ⟩, μM	DOC _b , μM
0–40	2.49	138	20.80 ± 1.3	124.57 ± 9.3	9.25 ± 0.79	20	0.73–14.78	5.39 ± 0.86
60–100	0.90	87	11.47 ± 0.7	30.11 ± 5.0	3.38 ± 0.46	9	0.40–3.00	1.45 ± 0.25
500	−0.25	22	4.35 ± 0.4	3.31 ± 0.8	1.10 ± 0.29	4	0.12–1.11	0.66 ± 0.21
1400–1500	−0.81	22	3.75 ± 0.6	1.76 ± 0.4	0.76 ± 0.18	5	0.14–0.76	0.44 ± 0.10
1800–2200	−0.93	15	3.24 ± 0.5	1.16 ± 0.6	0.80 ± 0.44	5	0.14–0.59	0.27 ± 0.09
2300–2700	−1.00	14	3.35 ± 0.6	1.75 ± 0.5	0.93 ± 0.37	2	0.04–0.11	0.07 ± 0.04
3000–3300	−0.94	6	1.22 ± 0.2	1.52 ± 0.6	1.15 ± 0.60	–	–	–

^aT, temperature; N, number of samples; B, bacterial biomass and standard error (SE); P, bacterial production and SE; μ, specific growth rate and SE; n, number of DOC_l samples; ⟨DOC_l⟩, range of DOC_l-values; DOC_b, mean DOC_l-values and SE. P and B were measured in the Greenland Sea in June and August 1999. DOC_l was measured in August 1999.

bacterial biomass (B) is regulated by the bacterial carbon uptake (U) and the mortality (M). The bacterial mortality contributes to the DOC_b and the refractory DOC (DOC_r) pools with the fractions ϵ_b and ϵ_r , respectively. The remaining part of the mortality loss and a fraction of the bacterial carbon uptake determined by the yield (ω) are remineralized to DIC. DOC_r is transformed to DOC_b at the surface through photo-dissociation (L). The conservation equations for the different carbon pools in the microbial loop are given by:

$$\frac{\partial B}{\partial t} = \omega U - M \quad (1)$$

$$\frac{\partial \text{DOC}_b}{\partial t} = -U + \epsilon_b M + D + L \quad (2)$$

$$\frac{\partial \text{DOC}_r}{\partial t} = \epsilon_r M - L \quad (3)$$

$$\frac{\partial \text{DIC}}{\partial t} = (1 - \epsilon_b - \epsilon_r) M + (1 - \omega) U \quad (4)$$

In addition to the sinks and sources formulated in equations (1)–(4) the contribution from advective and diffusive transports also affect the distribution of the four state variables. The influence from these transports on shaping the global deep-sea DOC distribution is studied in section 4.

3.2. Bacterial Uptake

[9] The bacterial production (P), related to the bacterial uptake via the yield, can be described in terms of the specific growth rate (μ) and the bacterial biomass:

$$P = \omega U = \mu B \quad (5)$$

The temperature dependence of the bacterial metabolic activity can be characterized as:

$$\mu = \mu_0 Q_{10}^{\frac{T-T_0}{10}} \quad (6)$$

where $T_0 = 0^\circ\text{C}$ is a reference temperature and μ_0 is a temperature normalized specific growth rate which can depend on other limiting factors, as for example the substrate availability. The temperature dependence of bacterial activity is found to be characterized by a Q_{10} -factor within the range of 2–3 in large areas of the ocean [Pomeroy and Wiebe, 2001], and our growth experiments with mixed bacterial samples from the Greenland Sea gives a value of $Q_{10} = 3.0$ (M. Middelboe and C. Lundsgaard, Microbial activity in the Greenland Sea: The role of DOC lability, mineral nutrients and temperature, submitted to *Aquatic*

Microbial Ecology, 2002). We use this value as representative for the temperature dependence of the bacterial uptake in the microbial loop. The temperature dependence of the bacterial carbon uptake in the model is based on our observations in the Greenland Sea. This temperature dependence has been found in previous studies of the bacterial activity in cold waters [Rivkin *et al.*, 1996] and the bacterial production has also been shown to correlate with both temperature and chlorophyll in the surface layers of the global ocean [Rivkin and Legendre, 2001]. From these experiments we also determine a yield factor of $\omega = 0.33$ which lies within the range of earlier reported values for the marine environment [del Giorgio and Cole, 1998]. We apply this value in the microbial loop.

[10] The specific growth rate decreases from 0.03 d⁻¹ at 100 m depth to a low value of about 0.01 d⁻¹ below 500 m (Table 1). The relative small vertical temperature gradient in the Greenland Sea can not account for this decrease in μ , and therefore we suggest that this change reflects a decrease in the substrate value of the released DOC. To account for this increase of the specific growth rate in the upper ocean we model μ_0 as:

$$\mu_0 = \alpha \text{DOC}_b \quad (7)$$

where α is a substrate affinity of the bacterial uptake of DOC_b. In general, the bacterial uptake can be modeled by a Monod expression involving a maximum uptake rate and

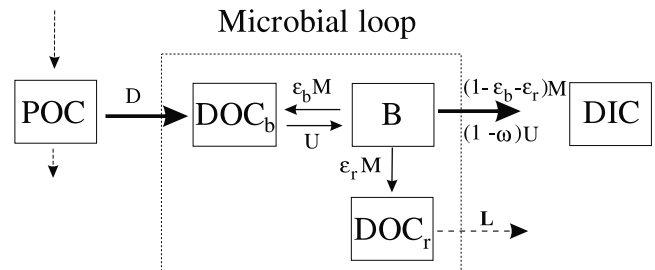


Figure 1. Microbial loop working in the water column below the euphotic zone is driven by the dissolution (D) of the sinking POC to DOC_b. The bacterial biomass (B) is regulated by the bacterial uptake (U) and the mortality (M). A fraction (ϵ_r) of the mortality ends as refractory DOC_r, which is transformed into labile DOC_b at the surface through photodissociation (L), a fraction is going into the DIC pool and a fraction (ϵ_b) is recycled back to DOC_b.

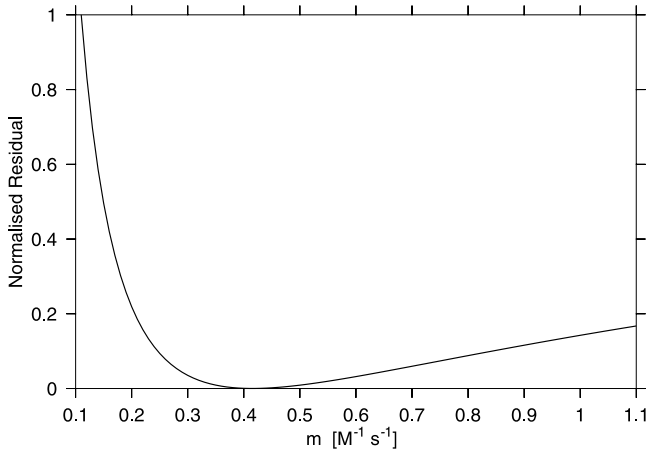


Figure 2. Normalized residual (R) given by equation (13) below 1000 m depth of the difference between the modeled bacterial biomass and the mean deep-sea distribution [Nagata *et al.*, 2000] as a function of the mortality constant (m) in equation (10).

a half saturation constant, but as bacterial uptake in the aphotic zone in the watercolumn is resource limited this expression can be linearized assuming a low concentration of DOC_b . The bacterial uptake can then finally be described as:

$$U = \frac{1}{\omega} \alpha \text{DOC}_b Q_{10}^{\frac{T-T_0}{10}} B \quad (8)$$

The yield and temperature dependence of the bacterial uptake are well studied components of the bacterial metabolism, whereas the substrate affinity of deep-sea DOC is largely unknown. Therefore we consider the sensitivity of the microbial loop to this parameter below.

3.3. Bacterial Mortality

[11] The bacterial abundance (N) below 1000 m depth in the equatorial, subtropical and subarctic areas in the North Pacific is well described as:

$$N(z) = N_{1000} \left(\frac{z}{z_d} \right)^a \quad (9)$$

where N_{1000} is the abundance at $z_d = -1000$ m depth and z is the vertical coordinate [Nagata *et al.*, 2000]. A uniform value of $a = -0.9$ characterizes the abundance in all these different locations, and this finding has implications for modeling the bacterial mortality in equations (1)–(4).

[12] The parameterization of the bacterial mortality in the deep ocean is not well constrained so we assume that the general form of this term can be described by:

$$M = m B^n \quad (10)$$

where m is a mortality constant and n is the power dependence of M on the bacterial biomass. The steady state solution of equations (1) and (2), which can be solved without considering the DIC and the DOC_r pools when the

contribution from photodissociation (L) in the surface layer is neglected, is then given by:

$$B = \sqrt[n]{\frac{D\omega}{m(1-\epsilon_b\omega)}} \quad (11)$$

As the source term for the microbial loop in the aphotic zone (D) we use the convergence of the vertical flux of POC found from sediment trap studies:

$$D = F_0 \frac{b}{z_0} \left(\frac{z}{z_0} \right)^{b-1} \quad (12)$$

where F_0 is the particulate flux at the bottom of the surface mixed layer at the depth z_0 , and we use a value of $b = -0.86$ which has been found to fit observations in large areas of the ocean [Martin *et al.*, 1987]. Together with the observed power dependence of bacterial abundance from Nagata *et al.* [2000], this parameterization of D constrains the mortality term to be related to the bacterial biomass with $n = 2$ resulting in a power dependence of the bacterial biomass given by: $a = \frac{1}{n}(-1-b) = -0.93$, close to the observed value of $a = -0.9$.

[13] The steady state solution obtained by using the estimated global mean value of new production (F_0) of $1.53 \text{ mol C m}^{-2} \text{ yr}^{-1}$ [Martin *et al.*, 1987] in equation (12) is fitted to the mean bacterial biomass distribution in the deep ocean observed by Nagata *et al.* [2000]. Using a representative value of $N_{1000} = 6.0 \cdot 10^{10} \text{ cells m}^{-3}$ and assuming a carbon content of $\nu_b = 20 \text{ fg C cell}^{-1}$ the best fit solution for the bacterial biomass is obtained, by minimizing the residual

$$R = \sum_{z < z_d} (B(z) - N(z) \nu_b)^2 \quad (13)$$

giving a best fit value of $m = 0.41 \text{ M}^{-1} \text{ s}^{-1}$ (Figure 2).

[14] The bacterial mortality is regulated both by viral lysis and grazing from higher trophic levels and these terms are assumed to amount equally to the mortality in equation (10) [Fuhrman and Noble, 1995]. We furthermore estimate that 95% of the bacterial mortality due to viral lysis is recycled as DOC_b whereas the uptake by bacterivores and the subsequent carbon flow through higher trophic levels only results in a recycling of 45% of the bacterial biomass as DOC_b . This gives a value of the recycling coefficient $\epsilon_b = 0.5 (0.95 + 0.45) = 0.7$ in the microbial loop, whereas the remaining part of the mortality is respired as DIC or degraded into the refractory DOC -pool [Ogawa *et al.*, 2001] through the term ϵ_r , which is constrained by the observed $\text{DOC}-\Delta^{14}\text{C}$ (see section 4).

3.4. Steady State Solutions

[15] The steady state solution of the bacterial biomass and DOC_b in the microbial loop (equations (1) and (2)) can be calculated for a given vertical temperature distribution and using the dissolution profile of POC given in equation (12) (Figure 3). Here we use a value for the substrate affinity of $\alpha = 0.6 \cdot 10^{-3} (\mu\text{M d})^{-1}$. The sensitivity of the temperature dependence of the bacterial biomass is illustrated by solving the equations for two different temperature profiles which represents the cold conditions at high latitudes and the global averaged temperature conditions in

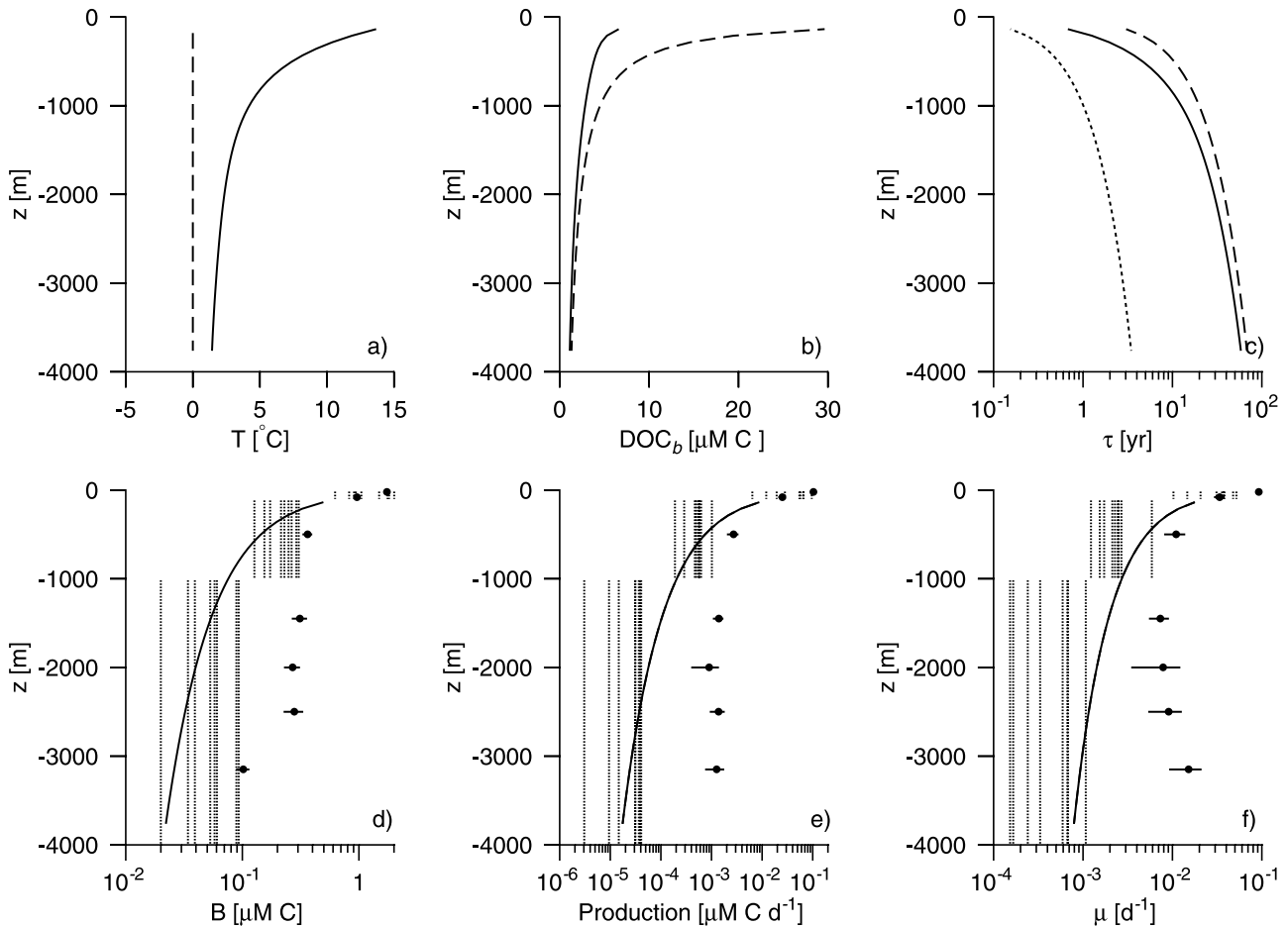


Figure 3. (a) Steady state solutions of equation (1) using the global mean flux of new production and the dissolution profile of POC from *Martin et al.* [1987] (see text) in a case with the global mean vertical temperature distribution (full lines) and a case with a constant temperature of 0°C (dashed lines). (b) Steady state solution of DOC_b and (c) turnover time (τ) for the DOC_b -pool and the bacterial biomass (dotted line). (d) Solution for the bacterial biomass, (e) bacterial production, and (f) specific growth rate for the two cases. Measurements and standard errors of B , P and μ from the Greenland Sea are shown (bullets) and the ranges reported by *Nagata et al.* [2000] for the northern Pacific are shown in the depth ranges 0–100 m, 100–1000 m, and 1000–4000 m (dotted vertical lines).

the watercolumn, respectively. The deep-sea DOC_b concentration of about 1 μM increases towards the values near the surface of about 6 μM and 29 μM in the warm and cold case, respectively.

[16] The turnover time of DOC_b increases from 3.0 yr at 100 m depth to 68 yr at 3800 m depth when the temperature is 0°C in the whole water column, whereas the solution for a case using the global mean vertical temperature distribution [*Levitus et al.*, 1994] results in a turnover time for DOC_b of 0.6 yr at 100 m depth increasing to 58 yr at 3800 m depth, showing the significance of the temperature dependence of the bacterial carbon demand in the upper part of the water column. These long timescales in the deep ocean imply that the DOC_b -pool can interact with the large scale ocean circulation, in particular in cold areas at high latitudes where the mixing between surface and deep waters is dominated by convection during winter time. Adding vertical mixing to the solutions would result in higher deep-sea DOC_b levels for the cold solution and therefore this temper-

ature dependence could explain the observed high deep-sea concentration of DOC in the North Atlantic.

[17] The steady state solution for B and P are independent of the temperature as shown in equation (11). The solutions for B , P and μ fall within the ranges reported by *Nagata et al.* [2000], whereas our measured values from the Greenland Sea are about an order of magnitude higher (Figure 3d–3f). This discrepancy could be explained by a higher level of DOC_b in the deep ocean at high latitudes, as shown in section 4, because this would result in higher values of B , P and μ .

[18] The steady state solution of DOC_b depends inversely on the substrate affinity (α) as:

$$DOC_b = \frac{m}{\omega \alpha Q_{10}^{\frac{T-T_0}{10}}} B \quad (14)$$

For a substrate affinity of about $10^{-3} (\mu\text{M})^{-1}$ the mean concentration of DOC_b in the watercolumn between 100 and 3800 m depth is 1.7 μM and 2.7 μM for the warm and cold

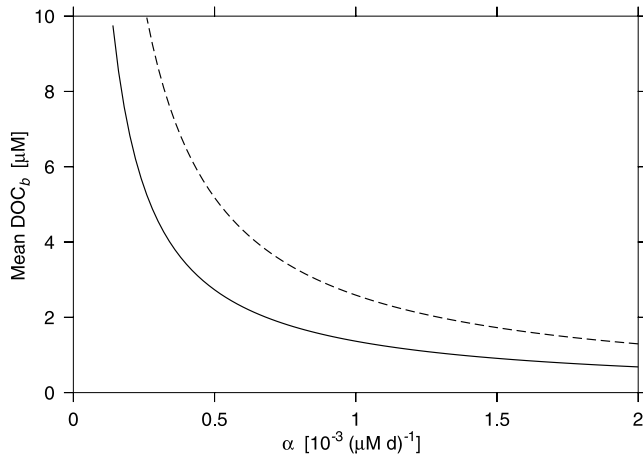


Figure 4. Mean vertical integrated steady state concentration of DOC_b in the depth range 100–3800 m of the microbial loop as a function of the substrate affinity (α). Solutions are shown for the global mean vertical temperature distribution (solid line) and for a constant temperature of 0°C in the whole water column (dashed line) and assuming the same new production and dissolution profile of POC as in Figure 3.

case, respectively (Figure 4). For low values of α of about $10^{-4} (\mu\text{M})^{-1}$ the total pool of DOC_b for the two temperature distributions increase to more than $10 \mu\text{M}$ whereas the total DOC_b -pool is reduced to about $1 \mu\text{M}$ when α approaches $2 \cdot 10^{-3} (\mu\text{M})^{-1}$. This sensitivity of the total DOC_b pool to the value of α is used to constrain α by the modeled global distribution of DOC_b , as discussed below.

4. Global Model Results

[19] To examine the possible interaction between the deep-sea DOC-pool and the large-scale circulation, the

microbial loop was implemented in a general ocean circulation model HAMOCC2 [Maier-Reimer, 1993; Archer *et al.*, 2000] which has a resolution of about 3.5° latitude \times 3.5° longitude and 11 vertical layers with increasingly resolution from the bottom towards the 50 m thick surface layer. The tracer field is integrated with a time step of 1 year and transported by the annual mean circulation. New production is regulated by surface nutrients, light and iron. A fraction of 17% of new production accumulates in the surface ocean as DOC_b and is subsequently mixed out of the euphotic zone [Hansell and Carlson, 1998b] and the rest is exported as sinking POC. The bacterial biomass is assumed stationary as the turnover time for the bacterial carbon pool is about 1 year in the model, in accordance with estimates of the turnover time of the deep-sea bacterial biomass (Dufour and Torr ton, 1996). The equations in the microbial loop are integrated within each time step with a fourth order Runge-Kutta algorithm. The model is integrated for 20,000 years to reach deep ocean $\text{DOC}-\Delta^{14}\text{C}$ steady state.

4.1. DOC and Bacterial Biomass

[20] The global averaged distribution of DOC increases from a deep value of about $43 \mu\text{M}$ below 3000 m to about $48 \mu\text{M}$ at the surface, whereas the refractory component is relatively constant throughout the water column with a value of about $41 \mu\text{M}$ (Figure 5a). At the surface the DOC_r decreases due to the transformation of DOC_r to DOC_b through photodissociation. The vertical distribution of DOC_b increases from a deep value of about $1 \mu\text{M}$ below 3000 m to a surface value of about $6 \mu\text{M}$. The sources of DOC_b in the surface layer only includes a small fraction of the primary production ($\sim 17\%$ of NP) and this is the reason for the relatively low DOC_b concentration in the mixed layer (Figure 5b). The majority of this surface DOC pool has a residence time of less than one year and therefore it will not influence the deep sea DOC distribution but only the upper few hundred meters of the water column.

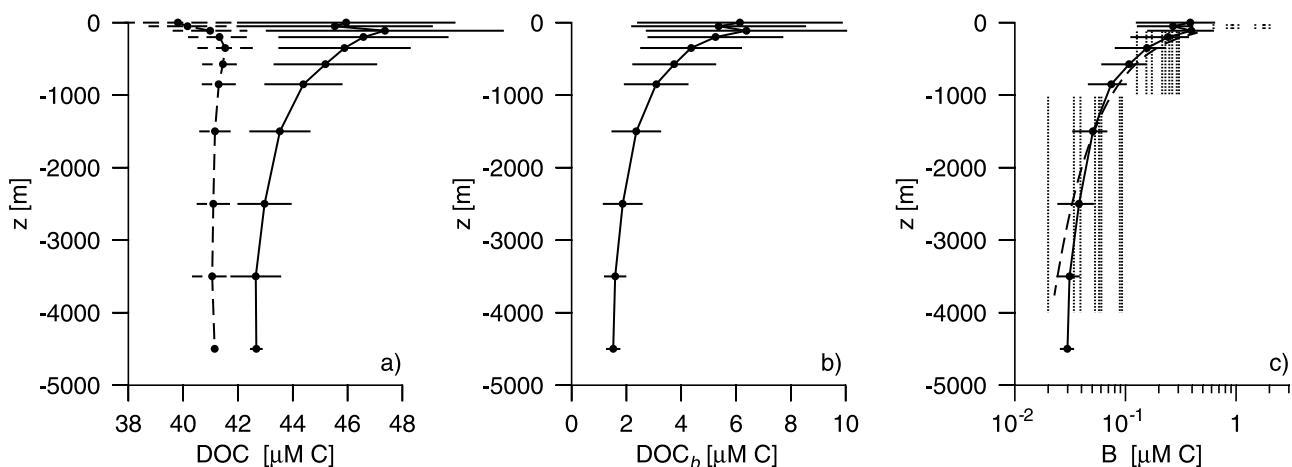


Figure 5. (a) Globally averaged HAMOCC2 model solution of DOC_r (dashed line) and total $\text{DOC} = \text{DOC}_r + \text{DOC}_b$ (solid line) and (b) the globally averaged distribution of DOC_b . (c) Globally averaged bacterial biomass (solid line) and the reference profile based on equation (9) from the observations of Nagata *et al.* [2000] (dashed line). The error bars show the standard deviation of the mean value at each vertical level. The ranges reported by Nagata *et al.* [2000] for the northern Pacific are shown in the depth ranges 0–100 m, 100–1000 m, and 1000–4000 m (dotted vertical lines).

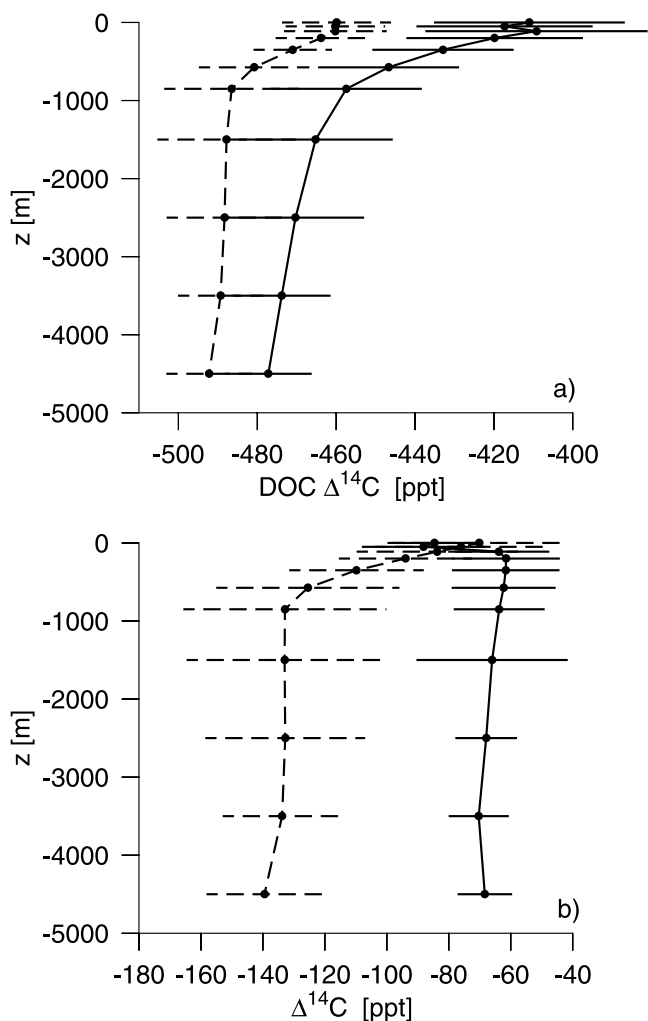


Figure 6. (a) Globally averaged HAMOCC2 model solution of the total $\text{DOC-}\Delta^{14}\text{C}$ (solid line) and the $\text{DOC}_r\text{-}\Delta^{14}\text{C}$ (dashed line). (b) Averaged distribution of $\text{DOC}_b\text{-}\Delta^{14}\text{C}$ (solid line) and $\text{DIC-}\Delta^{14}\text{C}$ (dashed line). The error bars show the standard deviation of the mean value at each vertical level.

[21] The globally averaged bacterial carbon biomass increases from a low concentration of about $3 \cdot 10^{-2} \mu\text{M}$ below 4000 m depth to a surface value of about $0.4 \mu\text{M}$ at 100 m depth (Figure 5c). This vertical distribution reflects the distribution of DOC_b , which is the substrate for the bacterial biomass. The global averaged value is in good accordance with the global mean vertical reference profile (Figure 5c, dashed line) based on the observations of Nagata *et al.* [2000] and described by equation (9). The observed range of the bacterial abundance in the North Pacific ranges within a factor of ten, including the influence from seasonal changes, so the global averaged model results of the bacterial biomass are well within the observed values of Nagata *et al.* [2000].

4.2. $\text{DOC-}\Delta^{14}\text{C}$ Distribution

[22] The observed deep ocean DOC concentration and the $\text{DOC-}\Delta^{14}\text{C}$ place a strong constraint on the fraction of the

bacterial mortality (ϵ_r) which contributes to DOC_r . The only sink of refractory DOC in the model is assumed to be due to photodissociation in the sunlit mixed layer where DOC_r is dissociated into DOC_b [Mopper *et al.*, 1991; Benner and Biddanda, 1998; Cherrier *et al.*, 1999]. The photodissociation is parameterized as a first-order decay process with a decay constant of 150 years [Yamanaka and Tajika, 1997], scaled with an incident light factor which also regulates new production [Bacastow and Maier-Reimer, 1990], thereby taking the latitudinal dependence of solar insolation into account [Moran and Zepp, 1997]. A value for ϵ_r of 2.4% leads to a global mean deep-ocean value below 500 m depth of $43 \pm 1.4 \mu\text{M}$ for DOC and -466 ± 19 ppt for $\text{DOC-}\Delta^{14}\text{C}$. The latter is within the observed range between -450 ppt and -500 ppt [Bauer *et al.*, 1992].

[23] The global averaged $\text{DOC-}\Delta^{14}\text{C}$ profile has a minimum value of about -480 ppt below 3000 m depth to a surface value of -410 ppt (Figure 6a). The refractory pool has a deep minimum value of about -490 ppt whereas the influence from newly produced organic matter in the main thermocline causes the $\text{DOC}_r\text{-}\Delta^{14}\text{C}$ to increase to about -460 ppt at the bottom of the surface layer. The gradual release of DOC from the sinking flux of POC has a ^{14}C -value which is determined by the $\text{DIC-}\Delta^{14}\text{C}$ value in the surface layer because this carbon pool is about two orders of magnitude larger than the DOC-pool. This influence causes the $\text{DOC}_b\text{-}\Delta^{14}\text{C}$ to be relatively constant throughout the water column with a value of about -60 ppt, which is close to the global averaged $\text{DIC-}\Delta^{14}\text{C}$ value in the surface layer (Figure 6b). The surface values of $\text{DOC}_b\text{-}\Delta^{14}\text{C}$ are relatively old because of the small amount of photodissociated DOC_r , which is transformed into DOC_b . Both old and newly produced DOC are incorporated into the bacterial biomass [Cherrier *et al.*, 1999]. So, in conclusion, the model is able to reproduce the observed ^{14}C age of bulk DOC in the deep ocean.

4.3. Global Deep-Sea DOC Distribution

[24] The mean DOC_b distribution below 1000 m depth in the model has the highest values of about $7 \mu\text{M}$ located in the Nordic Sea area where convective mixing is strongest in the model, and a general low concentration of DOC_b in the rest of the ocean between 1 and $3 \mu\text{M}$ (Figure 7a). The large new production in the strong upwelling zone in the eastern equatorial Pacific leads to a high deep-sea DOC_b concentration of about $4 \mu\text{M}$. The vertical mean concentration of DOC below 1000 m in the Atlantic shows significantly elevated levels in the northern North Atlantic of $48.0 \pm 1.1 \mu\text{M}$ (Figure 7b), within the errorbars of earlier reported values of $48.1 \pm 0.3 \mu\text{M}$ [Hansell and Carlson, 1998a]. Throughout the rest of the ocean the modeled deep-sea DOC concentration has a relatively constant level of about $43 \mu\text{M}$. The DOC_r concentration is almost constant with a mean value of $41.2 \mu\text{M}$ due to its long residence time. In the northern North Atlantic the deep DOC_r -levels are slightly lower due to the large vertical mixing with low photodissociated surface DOC_r . This model cannot explain the low values of about $39 \mu\text{M}$ and $34 \mu\text{M}$ (not shown) observed in the subtropical and northern North Pacific respectively [Hansell and Carlson, 1998a; Druffel and

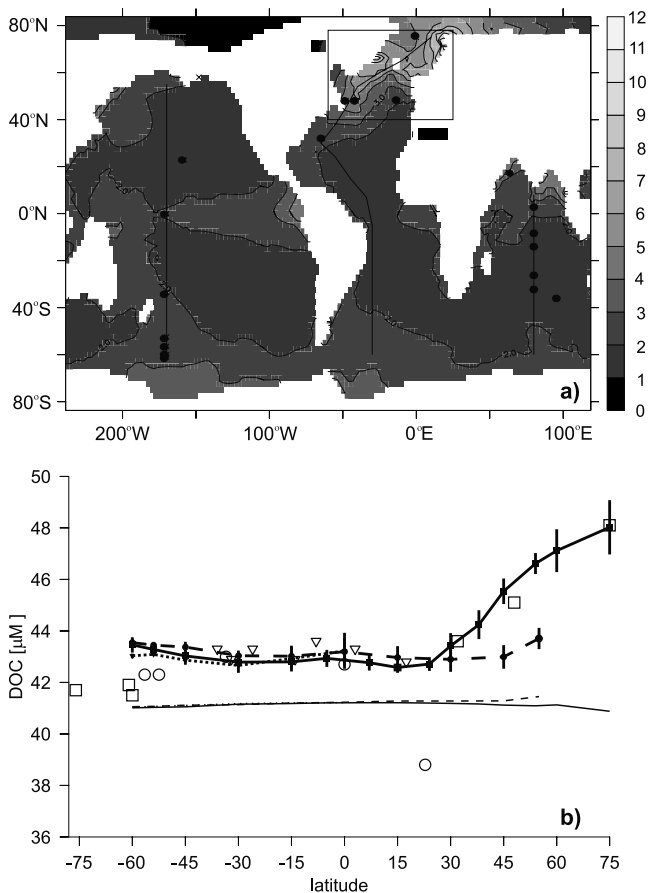


Figure 7. (a) Model solution of the vertical mean concentration of DOC_b [μM] below 1000 m depth. (b) The vertical mean integrated total DOC concentration below 1000 m in the Atlantic (red solid boxes, solid line), Indian (orange solid triangles, solid line) and Pacific Ocean (blue solid circles, solid line) as a function of latitude. The corresponding DOC_r concentrations are shown with thin lines. Model means and standard deviations are from 5° latitude \times 5° longitude rectangles centered along the tracks in each of the ocean basins shown in Figure 7a (black lines). Observations of deep-ocean DOC are from *Hansell and Carlson [1998a]* for the Atlantic (red open boxes), Pacific (blue open circles) and the Indian ocean (orange open triangles) and the corresponding locations are shown with red dots in Figure 7a. The red square in the northern North Atlantic refers to Figure 9. See color version of this figure at back of this issue.

Bauer, 2000]. Additional sinks or sources would have to be included to account for the low deep-sea DOC concentrations in these areas (see section 5).

[25] The concentration of the bacterial biomass and the bacterial production is significantly higher in the northern North Atlantic than in the North Pacific (Figure 8). The modeled *B* and *P* distributions in the North Pacific falls within the ranges reported by *Nagata et al. [2000]*. The observations in the Greenland Sea of *B* and *P* was made during the productive summer season and therefore the

annual averaged values would be lower by a factor of 2 or more, in consistency with the model results. The higher deep-sea specific growth rate in the North Atlantic can not be explained by the about 3°C lower deep-sea temperature there but is due to the larger concentration of DOC_b .

[26] The bacterial carbon uptake depends upon the quality of the available substrate which is regulated by the substrate affinity α in the microbial loop. A value of $\alpha = 0.6 \cdot 10^{-3} (\mu\text{M d})^{-1}$ is used here and gives a DOC_b concentration in the North Atlantic in agreement with observations. The DOC_b distribution is sensitive to lower values of α (compare Figure 4), such that a 50% lower value of α would result in a DOC_b pool about twice as large, whereas the sensitivity is less pronounced for higher values of α . An integration of the general circulation model was carried out with a doubling of α and this resulted in a decrease of the global deep-sea DOC_b concentration of about $1 \mu\text{M}$ and a drop of the elevated northern North Atlantic concentration to about $4 \mu\text{M}$. Few long-term incubation experiments with marine deep-sea DOC samples have been carried out [*Hopkinson et al., 1997*], but such experiments could provide information about the substrate dependent bacterial uptake and could constrain the unknown parameter α .

[27] The significance of the temperature dependence and circulation for the mean deep-sea DOC_b distribution below 500 m is reflected in the high correlation ($r \sim 0.74$) between new production (NP) and the DOC_b when the northern North Atlantic is disregarded compared to the case when this area is included ($r \sim 0.54$) in the analysis of the model data (Figure 9). To illustrate the influence of the temperature on the DOC_b distribution two integrations were carried out with the temperature in the microbial loop fixed to the global mean vertical temperature distribution (as shown in Figure 3a, solid line) and with the temperature fixed to 0°C (Figure 3a, dashed line). In the case with the global mean vertical temperature profile, the global DOC_b concentration correlates well with NP ($r \sim 0.78$) whereas the extreme case with a constant temperature of 0°C results in high concentrations of DOC_b in the northern North Atlantic and thereby a low correlation between DOC_b and NP ($r \sim 0.46$).

[28] The implications of the model results can be summarized as: Low surface temperatures at high latitudes cause a relatively long residence time of DOC_b in the upper part of the water column (0–1000 m). Large vertical mixing and the formation of deepwater in the northern North Atlantic transport DOC_b deeper into the water column and this leads to elevated concentrations of DOC_b in the North Atlantic region. The high deep-sea concentration of DOC_b also causes a higher concentration of *B* and a larger *P* than seen elsewhere in the ocean.

5. Discussion

[29] The focus of this study is the biodegradable part of the DOC-pool in the aphotic zone, which we estimate to account for 2–15% of the total DOC in the water column with the highest fraction in the subpolar areas and in areas with a high export production. DOC released from sinking aggregates through bacterial mediated enzymatic hydrolysis is an important substrate source for the free-living bacteria in

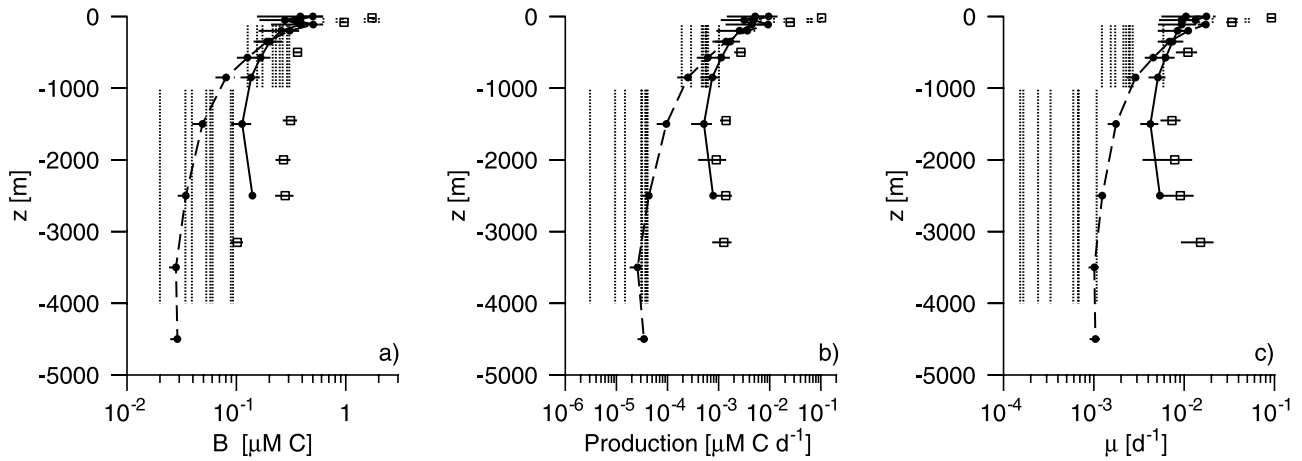


Figure 8. (a) Bacterial biomass, (b) bacterial production, and (c) the specific growth rate for the North Atlantic region ($55^{\circ}\text{N}:75^{\circ}\text{N}$, $40^{\circ}\text{W}:20^{\circ}\text{E}$; full line, bullets) and the North Pacific region ($55^{\circ}\text{N}:75^{\circ}\text{N}$, $40^{\circ}\text{W}:20^{\circ}\text{E}$; dashed line, bullets) in the model. The error bars shows the standard deviation. Also shown are the ranges reported by Nagata *et al.* [2000] for the North Pacific (dotted vertical lines) and the observed values in the Greenland Sea (boxes with standard deviation).

the ocean interior [Cho and Azam, 1988; Simon *et al.*, 1992; Nagata *et al.*, 2000]. Here we present observations of labile DOC from depths below 1400 m in the Greenland Sea which provide direct evidence for the particle associated transport of DOC. The incubation experiments were carried out during one week at 20°C . Using the temperature dependence of the bacterial uptake, characterized by $Q_{10}=3.0$, this would correspond to the bacterial uptake during 9 weeks at 0°C . A possible source of this deep-sea labile DOC-pool could be the transport associated with convective activity which reaches 1000–2000 m depth in the late winter [Lherminier *et al.*, 1999]. However, the measured turnover rates of DOC_l imply that any labile

DOC transported to 1000–2000 m depth by wintertime convection would have been consumed by bacteria in early spring, and therefore not be present below 1400 m in August. Therefore it is unlikely that the labile DOC is transported to intermediate depth levels by convective processes. Alternatively, the DOC could be transported to depth through diffusive or advective processes, but even the relatively high vertical diffusion observed in the central Greenland Sea of about $10^{-4} \text{ m}^2 \text{ s}^{-1}$ [Watson *et al.*, 1999] would only lead to vertical transports of less than 100 m during a 10-week period. The observation of deep-sea labile DOC can only be explained as DOC released from the sinking flux of POC.

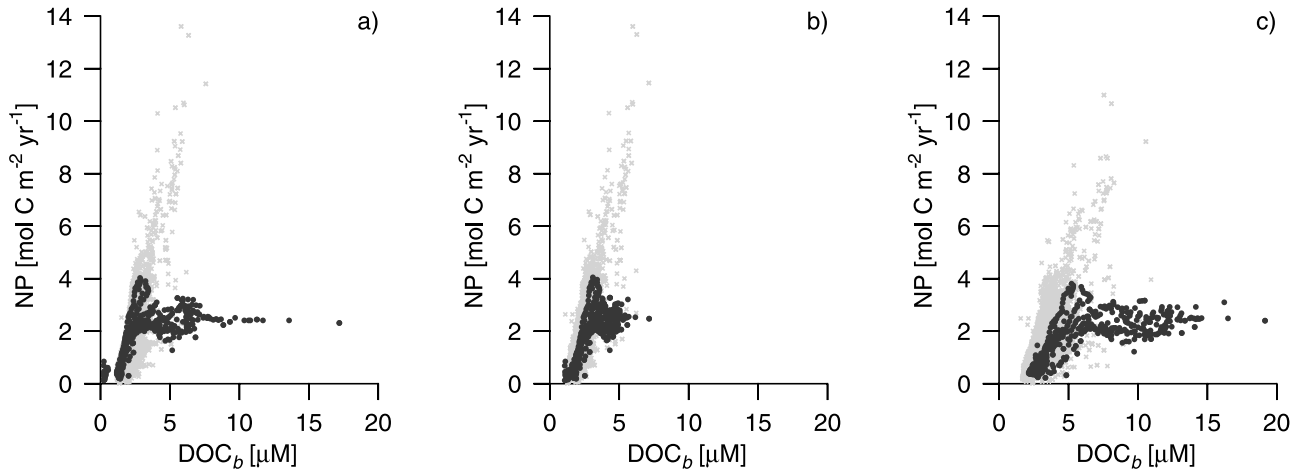


Figure 9. Scatterplot of new production (NP) versus the averaged DOC_b concentration below 500 m depth for the northern North Atlantic region (black) and the rest of the ocean (light shading). The results obtained by the microbial loop in (a) the standard case and for (b) the test case where the vertical global mean temperature distribution is used in the calculations of the bacterial uptake and (c) the case with a constant temperature of 0°C . The northern North Atlantic region is shown in Figure 7a.

[30] Convective activity during the cold winter season deepens the mixed layer in the Greenland Sea, and therefore the accumulation of DOC_b during the spring and summer seasons in the surface layer can potentially contribute to the total transport of DOC_b deep into the water column. The surface accumulation of DOC can account for a significant fraction of the new production in the area [Noji *et al.*, 1999], but the inverse correlation between the seasonal changes of DIC in the Greenland Sea and the corresponding changes of DOC in the Norwegian Sea indicates that most of the surface derived DOC is remineralized in the surface layer [Miller *et al.*, 1999]. From measurements of the bacterial production the estimated turnover time of the organic carbon in the surface layer (0–50 m) ranges within 8–91 days [Børsheim, 2000], and this also supports the view that surface derived DOC only makes a minor contribution to the deep-sea DOC in the area.

[31] Due to the limited data base which is currently available to establish parameterizations of the processes in the microbial loop which are valid on a global scale, the model was intentionally kept as simple as possible with a minimum number of free parameters. The critical parameters in the model are related to the sources and sinks of the bacterial biomass. We assume that 100% of the POC flux enters the DOC_b -pool, but this might be an overestimate of the actual source of DOC_b . Simon *et al.* [1992] estimated that the bacterial carbon uptake in the depth range of 80–600 m in the subarctic Pacific accounted for 41–172% of the POC flux measured in sediment traps, and Nagata *et al.* [2000] found that the bacterial carbon uptake accounted for 31–153% of the estimated POC flux in the deep North Pacific below 1000 m depth. These studies show that the sinking POC flux provides the substrate for the free-living bacterial biomass, but also they indicate that the assumption of a 100% release of POC to DOC_b could be an overestimation. Our results are not so sensitive to the fraction of the sinking POC-flux which enters the microbial loop because the mortality coefficient (m) in equation (10) is set by the level of the source term as seen from the steady state solution in equation (11) and the corresponding best fit solution defined from equation (13). A smaller fraction of the POC flux which enters the DOC_b -pool would cause a correspondingly lower value of m .

[32] Recent observations from the subtropical north Pacific, show that archaea makes up a significant fraction of the microbial biomass below 1000 m depth [Karner *et al.*, 2001]. The archaeal biomass is included in the observed estimates of the microbial biomass (which is simply referred to as the “bacterial biomass” above), but few experiments has been carried out on the archeal activity. Observations from the Pacific and the Mediterranean Sea show that archaea coexist with the bacteria and that they incorporate dissolved amino acids [Ouverney and Fuhrman, 2000]. These findings support the validity of our estimates of microbial production based on the incorporation of ^{14}C -leucine (Appendix A), but it is still unclear whether the archaeal metabolic activity can be described in terms of the parameterizations used for the bacterial activity.

[33] The nature of an additional deep-sea sink is presently unknown, but it could be a very slow decomposition of the DOC_r pool during its deep-sea transit from the Atlantic to the Pacific, for example due to hydrolysis, bacterial consumption or adsorption onto particulate material [Druffel *et al.*, 1996]. The $\text{DOC}-\Delta^{14}\text{C}$ age difference between the Sargasso Sea and the North Pacific is about 2000 years which is longer than the corresponding $\text{DIC}-\Delta^{14}\text{C}$ age difference of about 1500 years [Druffel *et al.*, 1992]. This difference between the age of the DIC and the DOC pool could in turn be explained if a slow deep-sea sink of the DOC_r preferentially removed the “youngest” part of the DOC_r pool. Such an “age”-fractionation has been observed to occur on much shorter timescales on riverine DOC transported into the ocean [Raymond and Bauer, 2001].

[34] The temperature dependence of the bacterial uptake also makes the oceanic DOC-pool sensitive to major changes in the thermal distribution in the ocean, as could have prevailed during other climatic regimes as for example the cold glacial periods. Two integrations were carried out where the temperature in the Q_{10} factor of the bacterial uptake were subtracted and added by 4°C , respectively. The global DOC_b concentration in the standard case is $2.8 \mu\text{M}$ and this increases (decreases) to $4.9 \mu\text{M}$ ($2.4 \mu\text{M}$) when 4°C is subtracted (added) corresponding to a change of 33 PgC (-6 PgC) of the global DOC_b inventory.

[35] In conclusion, a microbial loop based on the bacterial biomass in the aphotic zone can explain the elevated deep-sea concentration observed in the North Atlantic. Previous treatments of DOC [Yamanaka and Tajika, 1997; Six and Maier-Reimer, 1996; Murnane *et al.*, 1999] impose spatially uniform degradation timescales for DOC ranging from 0.5 to 11 years. In contrast, our results argue that the temperature-dependent, bacterially mediated DOC degradation has a significant impact on the distribution of DOC in the deep-sea. Through the workings of the bacterial biomass, the biological pump in the ocean achieves more degrees of freedom. Temperature dependent bacterial metabolism thus introduces a new degree of freedom to the global carbon cycle.

Appendix A. Measurements of DOC_b , B, and P

[36] DOC_l was determined in regrowth experiments as described by Søndergaard and Middelboe [1995]. In principle, all organisms except an inoculum of bacteria were removed from a water sample and the bacteria were allowed to grow to reach the carrying capacity with respect to organic carbon in the sample. DOC_l was estimated from the increase in bacterial biomass during incubation using an empirically determined growth efficiency of 0.24. The bacterial biomass was calculated from the bacterial abundance (measured by flow cytometry) using an empirically determined conversion factor of 23 fgC cell^{-1} . Bacterial growth efficiency and cell carbon content was determined in separate experiments. Here bacterial respiration was measured as oxygen consumption (using Winkler titration) and bacterial carbon production was measured as the increase in

POC collected on glass-fiber filters and measured as CO₂ after combustion at 650°C. Bacterial production was estimated from the incorporation of ¹⁴C-leucine [Chin-Leo and Kirchmann, 1988] using empirical conversion factors of 2060 gC mol⁻¹ leucine in June and 1280 gC mol⁻¹ leucine in August. Average values of leucine based data are presented here. More details about methods are given by M. Middelboe and C. Lundsgaard (Microbial activity in the Greenland Sea: The role of DOC lability, mineral nutrients and temperature, submitted to *Aquatic Microbial Ecology*, 2002).

[37] **Acknowledgments.** This work was funded by the Danish Natural Science Research Council, the Carlsberg Foundation and from the EU-project ORFOIS (contract EVK2-CT-2001-00100).

References

- Anderson, T. R., and P. J. B. Williams, A one-dimensional model of dissolved organic carbon cycling in the water column incorporating combined biological-photochemical decomposition, *Global Biogeochem. Cycles*, **13**, 337–349, 1999.
- Archer, D. E., E. T. Peltzer, and D. L. Kirchmann, A timescale for dissolved organic carbon production in equatorial Pacific surface waters, *Global Biogeochem. Cycles*, **11**, 435–452, 1997.
- Archer, D., A. Winguth, D. Lea, and N. Mahowald, What caused the glacial/interglacial atmospheric pCO₂ cycles?, *Rev. Geophys.*, **38**, 159–189, 2000.
- Bacastow, R., and E. Maier-Reimer, Ocean-circulation model of the carbon cycle, *Clim. Dyn.*, **4**, 95–125, 1990.
- Bauer, J. E., P. M. Williams, and E. R. M. Druffel, ¹⁴C activity of dissolved organic carbon fractions in the north-central Pacific and Sargasso Sea, *Nature*, **357**, 667–670, 1992.
- Benner, R., and B. Biddanda, Photochemical transformations of surface and deep marine dissolved organic matter: Effects on bacterial growth, *Limnol. Oceanogr.*, **43**, 1373–1378, 1998.
- Billen, G., P. Servais, and S. Becquevort, Dynamics of bacterioplankton in oligotrophic and eutrophic environments: Bottom-up or top-down control, *Hydrobiologia*, **207**, 37–42, 1990.
- Børshheim, K. Y., Bacterial production rates and concentrations of organic carbon at the end of the growing season in the Greenland Sea, *Aquatic Microb. Ecol.*, **21**, 115–123, 2000.
- Børshheim, K. Y., and S. M. Mykkestad, Dynamics of DOC in the Norwegian Sea inferred from monthly profiles collected during 3 years at 66°N, 2°E, *Deep Sea Res. Part I*, **44**, 593–601, 1997.
- Carlson, C. A., H. W. Ducklow, and A. F. Michaels, Annual flux of dissolved organic carbon from the euphotic zone in the northwestern Sargasso Sea, *Nature*, **371**, 405–408, 1994.
- Cherrier, J., J. E. Bauer, E. R. M. Druffel, R. B. Coffin, and J. P. Chanton, Radiocarbon in marine bacteria: Evidence for the ages of assimilated carbon, *Limnol. Oceanogr.*, **44**, 730–736, 1999.
- Chin-Leo, G., and D. L. Kirchmann, Estimating bacterial production in marine waters from simultaneous incorporation of thymidine and leucine, *Appl. Environ. Microbiol.*, **54**, 1934–1939, 1988.
- Cho, B. C., and F. Azam, Major role of bacteria in biogeochemical fluxes in the ocean's interior, *Nature*, **332**, 441–443, 1988.
- del Giorgio, P. A., and J. J. Cole, Bacterial growth efficiency in natural aquatic systems, *Annu. Rev. Ecol. Syst.*, **29**, 503–541, 1998.
- Druffel, E. R., and J. E. Bauer, Radiocarbon distributions in Southern Ocean dissolved and particulate organic matter, *Geophys. Res. Lett.*, **27**, 1495–1498, 2000.
- Druffel, E. R., P. M. Williams, J. E. Bauer, and J. R. Ertel, Cycling of dissolved and particulate organic matter in the open ocean, *J. Geophys. Res.*, **97**, 15,639–15,659, 1992.
- Druffel, E. R., J. E. Bauer, P. M. Williams, S. Griffin, and D. Wolgast, Seasonal variability of particulate organic radiocarbon in the northeast Pacific Ocean, *J. Geophys. Res.*, **101**, 20,543–20,552, 1996.
- Dufour, P., and J.-P. Torréton, Bottom-up and top-down control of bacterioplankton from eutrophic to oligotrophic sites in the tropical northeastern Atlantic Ocean, *Deep Sea Res., Part I*, **43**, 1305–1320, 1996.
- Fuhrman, J. A., and R. T. Noble, Viruses and protists cause similar bacterial mortality in coastal seawater, *Limnol. Oceanogr.*, **40**, 1236–1242, 1995.
- Hansell, D. A., and C. A. Carlson, Deep-ocean gradients in the concentration of dissolved organic carbon, *Nature*, **395**, 263–266, 1998a.
- Hansell, D. A., and C. A. Carlson, Net community production of dissolved organic carbon, *Global Biogeochem. Cycles*, **12**, 443–453, 1998b.
- Hopkinson, C. S., Jr., B. Fry, and A. L. Nolin, Stoichiometry of dissolved organic matter dynamics on the continental shelf of the northeastern U.S.A., *Cont. Shelf Res.*, **17**, 473–489, 1997.
- Karner, B. K., E. F. DeLong, and D. M. Karl, Arcaea dominance in the mesopelagic zone of the Pacific ocean, *Nature*, **409**, 507–510, 2001.
- Levitus, S., R. Burgett, and T. P. Boyer, *World Ocean Atlas*, vol. 4, *Temperature*, Natl. Oceanic and Atmos. Admin., U. S. Gov. Printing Off., Washington, D. C., 1994.
- Lherminier, P., J.-C. Gascard, and D. Quadfasel, The Greenland Sea in Winter 1993 and 1994: Preconditioning for deep convection, *Deep Sea Res., Part II*, **46**, 1199–1235, 1999.
- Maier-Reimer, E. U., Geochemical cycles in an ocean general circulation model: Preindustrial tracer distribution, *Global Biogeochem. Cycles*, **7**, 645–677, 1993.
- Martin, J. H., G. A. Knauer, D. M. Karl, and W. W. Broenkow, VERTEX: Carbon cycling in the northeast Pacific, *Deep Sea Res.*, **34**, 267–285, 1987.
- Middelboe, M., M. Søndergaard, Y. Letarte, and N. H. Borch, Attached and free-living bacteria: Production and polymer hydrolysis during a diatom bloom, *Microb. Ecol.*, **29**, 231–248, 1995.
- Miller, L. A., M. Chierici, T. Johannessen, T. T. Noji, F. Rey, and I. Skjelvan, Seasonal dissolved inorganic carbon variations in the Greenland Sea and implications for atmospheric CO₂ exchange, *Deep Sea Res., Part II*, **46**, 1473–1496, 1999.
- Mopper, K., X. Zhou, R. J. Kieber, D. J. Kieber, R. J. Sikorski, and R. D. Jones, Photochemical degradation of dissolved organic carbon and its impact on the oceanic carbon cycle, *Nature*, **353**, 60–62, 1991.
- Moran, M. A., and R. G. Zepp, Role of photoreactions in the formation of biologically labile compounds from dissolved organic matter, *Limnol. Oceanogr.*, **42**, 1307–1316, 1997.
- Murnane, R. J., J. L. Sarmiento, and C. L. Quéré, Spatial distribution of air-sea CO₂ fluxes and the interhemispheric transport of carbon by the oceans, *Global Biogeochem. Cycles*, **13**, 287–305, 1999.
- Nagata, T., H. Fukuda, R. Fukuda, and I. Koike, Bacterioplankton distribution and production in deep Pacific waters: Large-scale geographic variations and possible coupling with sinking particle fluxes, *Limnol. Oceanogr.*, **45**, 426–435, 2000.
- Noji, T. T., F. Rey, L. A. Miller, K. Y. Børshheim, and J. Urban-Rich, Fate of biogenic carbon in the upper 200 m of the central Greenland Sea, *Deep Sea Res., Part II*, **46**, 1497–1509, 1999.
- Ogawa, H., Y. Amagai, I. Koike, K. Kaiser, and R. Benner, Production of refractory dissolved organic matter by bacteria, *Science*, **292**, 917–920, 2001.
- Opsahl, S., and R. Benner, Distribution and cycling of terrigenous dissolved organic matter in the ocean, *Nature*, **386**, 480–482, 1997.
- Opsahl, S., R. Benner, and R. M. W. Amon, Major flux of terrigenous dissolved organic matter through the Arctic Ocean, *Limnol. Oceanogr.*, **44**, 2017–2023, 1999.
- Ouverney, C. C., and J. A. Fuhrman, Marine planktonic archaea take up amino acids, *Appl. Environ. Microbiol.*, **66**, 4829–4833, 2000.
- Pomeroy, L. R., and W. J. Wiebe, Temperature and substrates as interactive limiting factors for marine heterotrophic bacteria, *Aquat. Microb. Ecol.*, **23**, 187–204, 2001.
- Proctor, L. M., and J. A. Fuhrman, Roles of viral infection in organic particle flux, *Mar. Ecol.*, **69**, 133–142, 1991.
- Raymond, P. E., and J. E. Bauer, Riverine export of aged terrestrial organic matter to the North Atlantic Ocean, *Nature*, **25**, 497–500, 2001.
- Reid, J., and R. Lynn, On the influence of the Norwegian-Greenland and Weddel Seas upon the bottom waters of the Indian and Pacific oceans, *Deep Sea Res.*, **18**, 1063–1088, 1971.
- Rivkin, R. B., and L. Legendre, Biogenic carbon cycling in the upper ocean: Effects of microbial respiration, *Nature*, **291**, 2398–2400, 2001.
- Rivkin, R. B., M. R. Anderson, and C. Lajzerowicz, Microbial processes in cold oceans, 1, Relationship between temperature and bacterial growth rate, *Aquat. Microb. Ecol.*, **10**, 243–254, 1996.
- Simon, M., N. A. Welschmeyer, and D. L. Kirchman, Bacterial production and the sinking flux of particulate organic matter in the subarctic Pacific, *Deep Sea Res., Part I*, **39**, 1997–2008, 1992.
- Six, K. D., and E. Maier-Reimer, Effects on plankton dynamics on seasonal carbon fluxes in an ocean general circulation model, *Global Biogeochem. Cycles*, **10**, 559–583, 1996.

- Smethie, W. M., A. Rana, A. Putzka, and E. P. Jones, Tracing the flow of North Atlantic Deep Water using chlorofluorocarbons, *J. Geophys. Res.*, *105*, 14,297–14,323, 2000.
- Smith, D. C., M. Simon, A. L. Alldredge, and F. Azam, Intense hydrolytic enzyme activity on marine aggregates and implications for rapid particle dissolution, *Nature*, *359*, 139–142, 1992.
- Søndergaard, M., and M. Middelboe, A cross-system analysis of labile dissolved organic carbon, *Mar. Ecol. Progr. Ser.*, *118*, 283–294, 1995.
- Stedmon, C. A., and S. Markager, The optics of chromophoric dissolved organic matter (CDOM) in the Greenland Sea: An algorithm for differentiation between marine and terrestrially derived organic matter, *Limnol. Oceanogr.*, *46*, 2087–2093, 2001.
- Watson, A. J., et al., Mixing and convection in the Greenland Sea from a tracer-release experiment, *Nature*, *401*, 902–904, 1999.
- Yamanaka, Y., and E. Tajika, Role of dissolved organic matter in the marine biogeochemical cycle: Studies using an ocean biogeochemical general circulation model, *Global Biogeochem. Cycles*, *11*, 599–612, 1997.

D. Archer, Department of Geophysical Sciences, 5734 S. Ellis Avenue, University of Chicago, Chicago, IL 60637, USA. (d-archer@uchicago.edu)
J. Bendtsen and C. Lundsgaard, National Environmental Research Institute, Frederiksborgvej 399, Postbox 358, DK-4000 Roskilde, Denmark. (job@dmu.dk; clu@dmu.dk)

M. Middelboe, Marine Biological Laboratory, University of Copenhagen, Strandpromenaden 5, DK-3000Helsingør, Denmark. (mmiddelboe@zi.ku.dk)

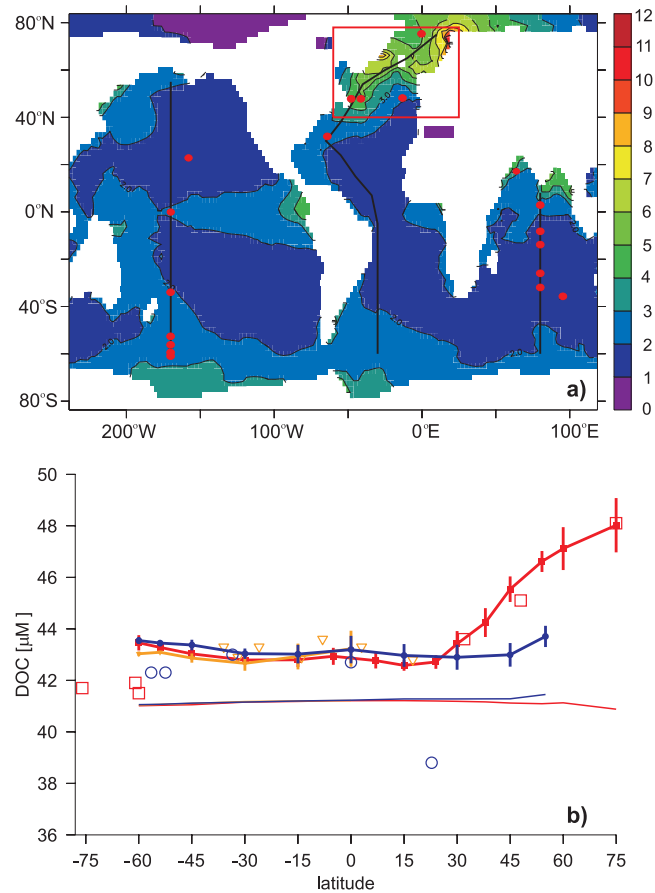


Figure 7. (a) Model solution of the vertical mean concentration of DOC_b [μM] below 1000 m depth. (b) The vertical mean integrated total DOC concentration below 1000 m in the Atlantic (red solid boxes, solid line), Indian (orange solid triangles, solid line) and Pacific Ocean (blue solid circles, solid line) as a function of latitude. The corresponding DOC_c concentrations are shown with thin lines. Model means and standard deviations are from 5° latitude \times 5° longitude rectangles centered along the tracks in each of the ocean basins shown in Figure 7a (black lines). Observations of deep-ocean DOC are from *Hansell and Carlson* [1998a] for the Atlantic (red open boxes), Pacific (blue open circles) and the Indian ocean (orange open triangles) and the corresponding locations are shown with red dots in Figure 7a. The red square in the northern North Atlantic refers to Figure 9.